

OPEN ACCESS

EDITED BY

Olivier Rodrigues, École d'Ingénieurs de PURPAN, France

REVIEWED BY

Dongchao Ji,

Shandong University of Technology, China Wanwan Liang,

Chinese Academy of Agricultural Sciences,

*CORRESPONDENCE

Benoit Poinssot

■ benoit.poinssot@inrae.fr

RECEIVED 15 September 2025 ACCEPTED 27 October 2025 PUBLISHED 27 November 2025

CITATION

Villette J, Marzari T, Landry D, Roudaire T, Klinguer A, Leborgne-Castel N, Vicedo C, Gasciolli V, Pouzet C, Lefebvre B, Héloir M-C and Poinssot B (2025) The *Vitis vinifera* receptor VvLYK6 negatively regulates chitintriggered immune responses and promotes fungal infections.

Front. Plant Sci. 16:1705961. doi: 10.3389/fpls.2025.1705961

COPYRIGHT

© 2025 Villette, Marzari, Landry, Roudaire, Klinguer, Leborgne-Castel, Vicedo, Gasciolli, Pouzet, Lefebvre, Héloir and Poinssot. This is an open-access article distributed under the terms of the Creative Commons Attribution License (CC BY). The use, distribution or reproduction in other forums is permitted, provided the original author(s) and the copyright owner(s) are credited and that the original publication in this journal is cited, in accordance with accepted academic practice. No use, distribution or reproduction is permitted which does not comply with these terms.

The *Vitis vinifera* receptor VvLYK6 negatively regulates chitin-triggered immune responses and promotes fungal infections

Jérémy Villette¹, Tania Marzari¹, David Landry², Thibault Roudaire¹, Agnès Klinguer¹, Nathalie Leborgne-Castel¹, Céline Vicedo², Virginie Gasciolli², Cécile Pouzet³, Benoît Lefebvre², Marie-Claire Héloir¹ and Benoit Poinssot^{1*}

¹Université Bourgogne Europe, Institut Agro, Institut National de la Recherche pour l'agriculture, l'alimentation et l'Environnement (INRAE), Unité Mixte de Recherche (UMR) Agroécologie, Dijon, France, ²Laboratory of Plant-Microbe-Environment Interactions (LIPME), Université de Toulouse, Institut National de la Recherche pour l'agriculture, l'alimentation et l'Environnement (INRAE), Centre National de la Recherche Scientifique (CNRS), Castanet-Tolosan, France, ³Toulouse Réseau imagerie (TRI) Fédération de Recherche Agrobiosciences, Interactions et Biodiversité (FR AIB) Imaging Platform Facilities, Fédération de Recherche Agrobiosciences Interactions et Biodiversité, Université de Toulouse, Centre National de la Recherche Scientifique (CNRS), UPS, Castanet-Tolosan, France

Introduction: Botrytis cinerea is recognized as one of the most damaging fungal pathogens affecting grapevine (Vitis vinifera), directly impacting both grape yield and wine quality. Identifying new genes involved in the interaction between V. vinifera and B. cinerea appears to be a promising strategy for enhancing grapevine resistance in future breeding programs. During pathogen infection, plasma membranelocalized pattern recognition receptors (PRRs) are responsible for detecting conserved microbe-associated molecular patterns (MAMPs). Among PRRs, members of the LysM receptor-like kinase family are well known to mediate the recognition of fungal MAMPs and trigger plant immune signaling pathways. Interestingly, a novel member of this receptor family, named VvLYK6, was identified in grapevine as the most highly upregulated during B. cinerea infection.

Methods: To investigate the role of VvLYK6 in plant immunity, we conducted overexpression studies in Arabidopsis thaliana and grapevine cell suspensions. **Results:** Overexpression of VvLYK6 led to a reduction in chitin-induced MAPK activation, decreased expression of defense-related genes, reduced callose deposition, and increased plant susceptibility to fungal pathogens in *A. thaliana*. **Discussion:** Based on these findings, we conclude that VvLYK6 acts as a negative regulator of chitin-triggered immune responses, suggesting its potential role as a susceptibility gene during fungal infections.

KEYWORDS

Vitis vinifera, MAMP, chitin hexamer, inhibition, plant immunity, fungal pathogens

Introduction

Grapevine (Vitis vinifera) is continuously exposed to intense pest pressure, including viruses, insects, oomycetes such as downy mildew (Plasmopara viticola), and fungi such as powdery mildew (Erysiphe necator) and grey mold (Botrytis cinerea). Although downy mildew and powdery mildew are known to be the most damaging diseases in vineyards, Botrytis cinerea still represents a significant risk, potentially causing yield losses of 20% to 50% (Rahman et al., 2024). Current strategies to mitigate the impact of these diseases rely heavily on chemical treatments. However, these treatments pose risks to both the environment and human health, prompting the development of alternative approaches for disease management in vineyards (Pathak et al., 2022). One such approach involves the identification of resistance (R) and susceptibility (S) genes (Qiu et al., 2015; Zaidi et al., 2018). The introgression of R genes into grapevine has been a key strategy for developing durable, disease-resistant varieties (Xiao et al., 2023). Notably, two members of the TIR-NB-LRR gene family from Muscadinia rotundifolia (a close related species of V. vinifera) have been identified as major R genes, conferring resistance to several important grapevine pathogens (Feechan et al., 2013). Interestingly, it has also been frequently observed that loss of function of S genes can lead to broad-spectrum resistance, making them attractive targets for breeding programs (Zaidi et al., 2018).

Another promising strategy involves triggering grapevine immunity by eliciting plant defense responses with bioproducts (Adrian et al., 2024). Plant innate immunity relies on two wellcharacterized defense signaling pathways (Boller and Felix, 2009). The first is microbe-associated molecular pattern (MAMP)-triggered immunity (MTI), also referred to as pattern-triggered immunity (PTI). The second is the effector-triggered immunity (ETI), which is activated upon recognition of pathogen-derived effectors by plant resistance proteins (Böhm et al., 2014; Zipfel, 2014). MTI represents the initial layer of plant immune defense, involving the recognition of conserved MAMPs released by invading microbes. These molecular patterns are detected by cell-surface pattern recognition receptors (PRRs), which initiate intracellular signal transduction cascades. This signaling typically involves phosphorylation events mediated by mitogenactivated protein kinases (MAPKs), ultimately leading to the activation of transcription factors and expression of defense-related genes. Depending on the nature and concentration of the MAMPs, various defense responses can be triggered, including callose deposition, production of phytoalexins (such as stilbenes in grapevine), and synthesis of pathogenesis-related (PR) proteins (Ahuja et al., 2012; Zhou and Zhang, 2020).

Plant PRRs are structurally diverse and encompass several protein families, classified based on the nature of their extracellular domains (Ngou et al., 2022). Among these, the Lysin motif receptor-like kinases (LysM-RLKs) and Lysin motif receptor-like proteins (LysM-RLPs) are well-characterized for their ability to perceive various polysaccharides, including chitooligosaccharides (COS), lipochitooligosaccharides (LCOs), and peptidoglycan (PGN). In all plant species, the LysM-RLK family is subdivided into two main groups: LYK receptors, which possess an active

kinase domain capable of transducing signals into the cell, and LYR receptors, which contain an inactive kinase domain and are presumed to act as co-receptors. In contrast, LysM-RLPs (also referred to as LYMs) lack a kinase domain entirely and are thought to function in ligand recognition without direct signal transduction (Buendia et al., 2018).

Chitin, a major structural component of fungal cell walls, is perceived by a complex of LysM-RLKs and LysM-RLPs at the plasma membrane, which together mediate signal transduction. In Arabidopsis thaliana, the LYR-type receptor AtLYK5, known for its high affinity for chitin oligomers, forms heterodimers with another LYR receptor, AtLYK4 (Wan et al., 2012; Cao et al., 2014; Xue et al., 2019). Despite their ability to bind chitin, the AtLYK4/5 complex cannot initiate intracellular signaling due to its inactive kinase domains. Instead, signal transduction relies on the recruitment of the LYK-type receptor AtCERK1, which possesses an active kinase domain but has relatively low affinity for chitin oligomers (Miya et al., 2007; Cao et al., 2014). In rice (Oryza sativa), the LYK-type receptor OsCERK1 plays a dual role in both immune and symbiotic signaling pathways (Zhang et al., 2021). For immune responses, OsCERK1 interacts with LysM-RLPs such as OsCEBiP, OsLYP4, and OsLYP6 to activate defense signaling upon chitin recognition (Shimizu et al., 2010; Ao et al., 2014). In contrast, during the establishment of arbuscular mycorrhizal (AM) symbiosis, OsCERK1 forms a complex with the LYR-type receptor OsMYR1 to mediate symbiotic signaling (He et al., 2019). These studies collectively highlight the central role of OsCERK1 in signal transduction, functioning across distinct biological contexts. The specificity of the signaling pathway depends on the nature of the ligand and its high-affinity interaction with its corresponding receptor.

Phylogenetic analyses have revealed well-conserved clades within the LysM receptor family, reflecting their functional specialization (Buendia et al., 2018). For example, the LYRIII C clade includes AtLYK5 and MtLYR4, which share a conserved function in the perception of chitin oligomers and play a role in MTI activation in A. thaliana and Medicago truncatula, respectively (Cao et al., 2014; Feng et al., 2019). Similarly, the LYRI A clade, which comprises OsMYR1 and SlLYK10, is functionally conserved in the perception of LCOs and is involved in the establishment of AM symbiosis in rice and tomato, respectively (Buendia et al., 2016; Girardin et al., 2019; He et al., 2019; Cullimore et al., 2023). In grapevine, recent studies support a similar model in which VvLYK1-1 and VvLYK1-2 (orthologs of AtCERK1), along with VvLYK5-1 (ortholog of AtLYK5), mediate chitin signaling. These LysM-RLKs have been shown to participate in chitin perception and to restore MAPK activation, defense gene expression, and pathogen resistance in A. thaliana mutants lacking functional chitin receptors (Brulé et al., 2019; Roudaire et al., 2023). Moreover, the formation of a receptor complex between VvLYK1-1 and VvLYK5-1 was found to be dependent on the presence of chitin oligomers. Interestingly, in grapevine, 16 LysM-RLK members have been identified and classified into 10 of the 11 phylogenetic clades defined by Buendia et al. (2018), suggesting broad diversification and potential functional specialization of this receptor family in the species.

In the present study, we investigated the role of VvLYK6, a member of the V. vinifera LYRI B LysM-RLK clade, which remains poorly characterized. Orthologs of VvLYK6 in various monocot and dicot species, including tomato, have been implicated in the establishment of AM symbiosis (Li et al., 2022; Ding et al., 2025). Interestingly, Brulé et al. (2019) reported that VvLYK6 was the most highly expressed LysM-RLK during B. cinerea infection in susceptible mature grape berries. Using functional genomics approaches, we demonstrated that VvLYK6 suppresses chitintriggered immune responses and increases plant susceptibility to three distinct fungal pathogens. Our findings suggest that VvLYK6 acts as a negative regulator of plant immunity, contributing to heightened susceptibility to grey mold. Therefore, VvLYK6 may be considered a novel S gene encoding a negative regulator of V. vinifera immune responses and could serve as a target for future breeding programs.

Materials and methods

Plant materials and growth conditions

A. thaliana wild-type (WT) Columbia (Col-0) ecotype, Atcerk1 mutant (GABI-Kat_096F09, allele Atcerk1-2; Gimenez-Ibanez et al., 2009), or transgenic lines Col-0-p35S::VvLYK6, Col-0-p35S:: VvLYK6-Green Fluorescent Protein, and Atcerk1-p35S::VvLYK6 were grown under a 10/14-h day/night cycle at 20°C/18°C. Transgenic lines were obtained by floral-dip transformation (Clough and Bent, 1998) of the Col-0 ecotype and Atcerk1 mutant lines with the coding sequence of VvLYK6 (Vitvi05g00623) amplified from complementary DNA (cDNA) of the susceptible Vitis vinifera cv. Marselan leaves and cloned into the pFAST R02 and pFAST R05 (Shimada et al., 2010). Transgenic seeds were selected with glufosinate (50 mg/L) and kanamycin (50 mg/L) selection for pFAST_R02 and pFAST_R05, respectively, and subsequently genotyped (Supplementary Figure S1). All experiments on A. thaliana were performed on the third selected homozygous line.

Cell cultures of *Vitis vinifera* cv. Marselan were maintained at 25°C under continuous light (30–40 µmol m⁻² s⁻¹) in liquid Nitsch-Nitsch (NN) medium (Nitsch and Nitsch, 1969) supplemented with 1 g/L casein hydrolysate, 400 µg/L 1-naphthaleneacetic acid, and 40 µg/L 6-benzylaminopurine. The cultures were kept in suspension by continuous shaking at 130 rpm, and were subcultured every 7 days at a 1:6 dilution ratio. For experiments, 7-day-old cultures were diluted twice with new medium. Grapevine cells were transformed by co-cultivation with *Agrobacterium tumefaciens* culture at an absorbance of 0.3 for 2 days. Cells were then transferred to NN medium with 0.7% agar, supplemented with 50 mg/L kanamycin for transformant selection and 250 mg/L cefotaxime to inhibit *Agrobacterium* growth. After 1 month, two independent lines expressing 35S-VvLYK6-GFP were selected.

Analysis of VvLYK6 gene expression in developmental and pathogen-infected grapevine tissues

Microarray and data analysis were performed as described in Kelloniemi et al. (2015) from grapevine (*V. vinifera cv. Marselan*) leaves and berries infected with *B. cinerea* and leaves infected by P. viticola. VvLYK6 expression profile of V. vinifera cv. Garganega berries, infected or not with *B. cinerea*, was obtained from the supplemental data of Lovato et al. (2019). Transcriptomic data highlighting differential VvLYK6 expression between pre-egression and egression states in V. vinifera cv. Pinot Noir infected with *B. cinerea* were obtained from Haile et al. (2020).

Phylogenetic analysis of the VvLYKs

Protein sequences for the LysM-RLK family were retrieved using BLAST searches, in which *A. thaliana* family members were used as query sequences against protein sequences from plant species detailed in Supplementary Table S1. A 1,000-bootstrap phylogenetic tree, comprising 96 protein sequences (Supplementary Table S1), was constructed with the maximum likelihood method and the JTT model (Jones et al., 1992). Alignment and phylogenetic analysis were performed with MEGA X software (Kumar et al., 2018).

Pathogen assays

The B. cinerea inoculum was produced by growing the strain BMM on solid medium (V8/2 tomato juice, 1% agar) in the dark to promote sporulation (Zimmerli et al., 2001). Conidia were isolated and concentrated in water to infect A. thaliana leaves at a final concentration of 5×10^4 conidia/mL, diluted in potato dextrose broth medium (PDB, 0.6%). Four-week-old Arabidopsis leaves were cut and maintained under survival conditions during B. cinerea infection. The A. brassicicola inoculum strain MIAE01824, originating from the Agroecology Unit collection (UMR1347, Dijon, France), was grown for 20 days on solid potato dextrose agar medium (PDA, 19 g $\rm L^{-1})$ supplemented with sucrose (20 g $\rm L^{-1})$ and CaCO₃ (30 g L⁻¹) at 20°C in the dark. Four-week-old Arabidopsis leaves were cut and maintained under survival conditions during A. brassicicola infection. Lesion surfaces caused by these two necrotrophic fungi were measured using ImageJ software (https://imagej.net/ij/).

Erysiphe necator assays were performed as described by Roudaire et al. (2023). Fungal structures were visualized using a Leica DMA light microscope (magnification \times 400). For each treatment, 100 germinated spores were evaluated. The percentage of successful epidermal cell penetration was determined based on the presence of a haustorium within the cell or the emergence of

secondary hyphae from the appressorium, as previously described by Roudaire et al. (2023). Three independent biological experiments were conducted.

with an Amersham ImageQuant800 (Cytiva, Laval, France). Quantification of MAPK intensity was normalized by total protein stained by Ponceau red using ImageQuant software.

Confocal microscopy

Confocal microscopy was performed using a Leica TCS SP8 multiphoton microscope with a \times 40 oil-immersion objective. Marselan suspension cells and leaf segments of *A. thaliana* lines expressing *VvLYK6* tagged with GFP were mounted directly or in ultrapure water between slide and coverslips, respectively, and observed. For plasma membrane staining, samples were incubated in 10 μ M FM4-64 for 10 min prior to observation. Fluorescent markers were excited with a 488-nm laser. GFP and FM4-64 emissions were bandpass filtered at 500–525 and 616–694 nm, respectively. Images were then treated with LAS X software.

Elicitors and plant treatment

In this study, we used as elicitors a purified hexamer (DP6) of chitin (GLU436, Elicityl, Crolles, France) at a concentration of 0.05 g/L and flagellin 22 (flg22) peptide from *Xanthomonas campestris* pv. campestris strain 305 (QRLSSGLRINSAKDDAAGLAIS) at 10⁻⁶ or 10⁻⁸ M, depending on the bioassay (Trdá et al., 2014). For *A. thaliana* treatments, 4-week-old plant leaves were preinfiltrated with ultrapure water and placed on a six-well plate containing ultrapure water for 4 h. Ultrapure water was then replaced by either ultrapure water (control) or elicitors, which were in contact with leaves for 10 min for MAPK activation and 1 h for real-time quantitative PCR (RT-qPCR) experiments, before freezing the samples in liquid nitrogen.

Grapevine cell suspensions were equilibrated at 0.1 g/mL and shaken under the same conditions as for their culture. Treatments were performed in a volume of 20 mL with a final concentration of 0.05 g/L chitin DP6. Cells were harvested in liquid nitrogen at 10 min posttreatment for MAPK activation and 1 h posttreatment for RT-qPCR analysis.

MAPK phosphorylation

For MAPK phosphorylation, treated *A. thaliana* leaves or grapevine cells were crushed in liquid nitrogen, and total proteins were extracted with a solution containing 50 mM HEPES (pH 7.5), 5 mM Ethylenediaminetetraacetic acid (EGTA) (pH 8.1), 5 mM Ethylenediaminetetraacetic acid, 1 mM Na₃VO₄, 50 mM β-glycerophosphate, 10 mM NaF, 1 mM phenylmethanesulfonyl fluoride, 5 mM dithiothreitol, and complete EDTA-free protease inhibitor cocktail (Roche, Boulogne-Billancourt, France). Phosphorylation of MAPKs was detected by immunoblotting of 25 μg total proteins using an anti-p42/44-phospho-ERK antibody (Cell Signaling Technology, Leiden, The Netherlands). The antibody signal was then revealed using ECL Prime (Cytiva, Laval, France) Western blotting detection reagent and imaged

Real-time quantitative PCR analysis

For RT-qPCR experiments, treated leaves or cells were crushed in liquid nitrogen, and total RNA was extracted with the SV Total RNA Isolation System with DNAse treatment (Promega, Madison, WI, USA). First-strand cDNAs were synthesized with the High-Capacity cDNA Reverse Transcription kit (Applied Biosystems, Waltham, MA, USA). RT-qPCR was performed in a ViiATM 7 Real-Time PCR system (Applied Biosystems, Waltham, MA, USA) with 10 ng cDNA and 1X GoTaq® qPCR Master Mix (Promega, Madison, WI, USA). Relative gene expression was assessed by taking into consideration the efficiency (E) of each reaction, calculated using the LinRegPCR quantitative PCR data analysis program (Ruijter et al., 2009). Gene expression values were normalized with two housekeeping genes: AtRHIP1 (At4g26410) and AtPTB1 (At3g01150) for RT-qPCR experiments on A. thaliana, and VvRPL18B (Vitvi05g00033) and VvVPS54 (Vitvi10g01135) for RT-qPCR assays on grapevine cells (Vitis vinifera cv. Marselan). All primers used are listed in Supplementary Table S2.

Callose deposition analysis

Four-week-old *Arabidopsis* were sprayed on both sides with either water (as a control) or chitin DP6 (0.05 g L⁻¹). Four days posttreatment, two leaves from three independent plants per condition were sampled and fixed in absolute ethanol for one night. Aniline blue staining was performed as detailed in Roudaire et al. (2023). Leaves were then observed on the adaxial side by epifluorescence microscopy under $\lambda_{\rm ex}=340$ –380 nm and $\lambda_{\rm em}=425$ nm, magnification \times 100, using a Leica DMRB microscope. Callose deposits were acquired for each condition using Nis Elements BR software (Nikon, Amstelveen, The Netherlands) with the DS-5Mc-U1 digital photomicrographic camera (Nikon, Amstelveen, The Netherlands). Image analysis was subsequently performed with the Fiji application, as described in Mason et al. (2020), using the Trainable Weka Segmentation plugin.

Transient expression for FRET-FLIM analysis

Transient expression in *Nicotiana benthamiana* leaves was previously described in Girardin et al. (2019) using *Agrobacterium* containing a cassette overexpressing either VvLYK1-1^{G328E} (Brulé et al., 2019) fused with a C-terminal Cyan Fluorescent Protein (CFP) alone, or with VvLYK6 or VvLYK5-1 (Roudaire et al., 2023) tagged with a C-terminal yellow fluorescent protein (YFP) (Karimi et al., 2005). The kinase-dead mutant version

of VvLYK1-1 (VvLYK1-1^{G328E}) was generated using the Quik Change Site-Directed Mutagenesis protocol (Liu and Naismith, 2008). FLIM was performed on an inverted LEICA DMi8 microscope equipped with a TCSPC system from PicoQuant Rudower Chaussee 29 (IGZ) 12489 Berlin, Germany. The excitation of the CFP donor at 440 nm was carried out by a picosecond pulsed diode laser at a repetition rate of 40 MHz, through an oil immersion objective (× 63, N.A. 1.4). The emitted light was detected by a Leica HyD detector in the 450-500 nm emission range. Images were acquired with acquisition photons of up to 1,500 per pixel. Data were acquired in three independent experiments and pooled. From the fluorescence intensity images, decay curves of CFP were calculated per pixel and fitted (using Poissonian maximum likelihood estimation) with either a doubleor tri-exponential decay model using the SymphoTime 64 software (PicoQuant, Berlin, Germany). The double-exponential model function was applied for donor samples containing only CFP present, whereas the tri-exponential model was used for samples containing CFP and YFP.

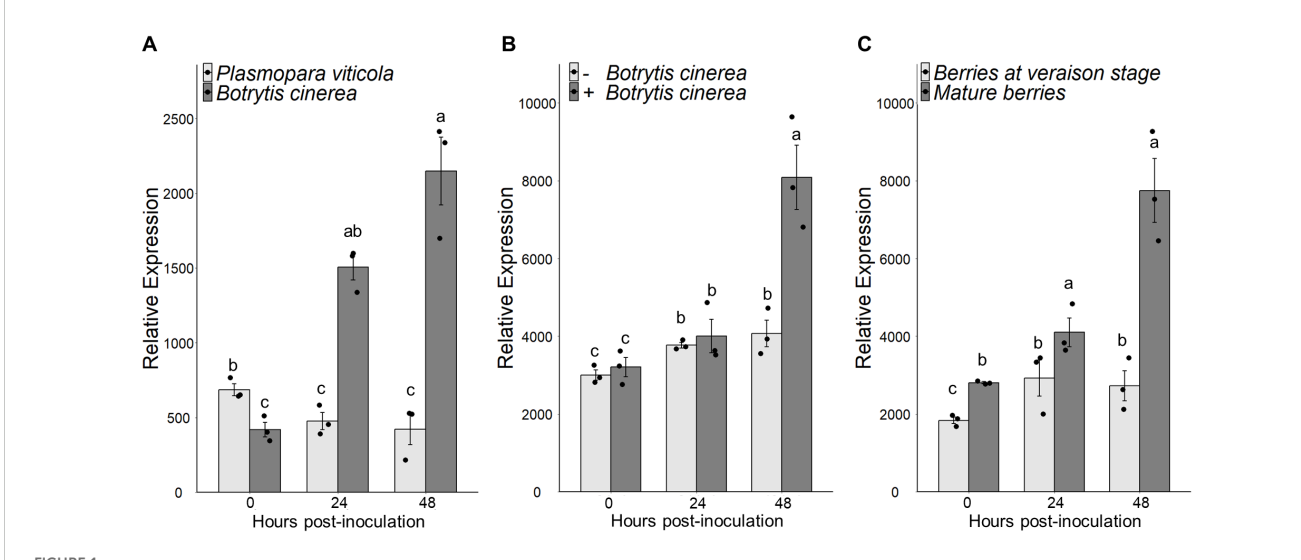
Co-immunopurification with VvLYK1-1

For co-immunopurification, the sequence coding VvLYK1- $1^{\rm G328E}$ was fused to a sequence coding a triple hemagglutinin (HA) tag. VvLYK1- $1^{\rm G328E}$ -HA and VvLYK6-YFP or VvLYK5-1-YFP were expressed in *N. benthamiana*. Leaf material was collected 3 days after infiltration, and co-immunopurification was performed

as described in Ding et al. (2024), except that anti-HA beads (Pierce Anti-HA Magnetic Beads, 88836) were used for purification, and anti-HA-HRP antibodies (Roche, Anti-HA-Peroxidase High affinity from rat IgG1, 12013819001) were used for Western blotting. Chitin DP6 (CO6) at 0.1 g/L was infiltrated into leaves before harvest and added to the IP buffer for protein solubilization and bead washes.

Microsomal fraction preparation and binding assay

Preparation of microsomal fraction and binding assays were previously described in Girardin et al. (2019). CO5- and CO7biotin were synthesized as detailed in Cullimore et al. (2023). Briefly, binding assays with CO5- and CO7-biotin were conducted on microsomal fractions in the binding buffer described in Girardin et al. (2019) for 1 h at 4°C. For Western blotting, proteins were separated by SDS-PAGE using homemade 6% polyacrylamide gels and transferred onto nitrocellulose membranes with a Trans-Blot system (Bio-Rad, Basel, Switzerland). The membranes were blocked for 1 h and incubated for 1 h with the following antibodies: α -GFP (11814460001, Roche, 1:3,000), followed by goat α -mouse-HRP (1706516, Bio-Rad, 1:10,000) or streptavidin-HRP (S911, Invitrogen, Waltham, MA, USA 1:3,000). The chemiluminescent signal from HRP was detected using the Chemidoc system (Bio-Rad, Basel, Switzerland).



VVLYK6 is induced during Botrytis cinerea infection on grapevine leaves and mature berries. (A) VVLYK6 expression profiles were analyzed at 0, 24, and 48 h postinoculation on leaves infected either by Botrytis cinerea or Plasmopara viticola. (B) VVLYK6 expression profiles were analyzed at 0, 24, and 48 h postinoculation on ripe berries infected or not with B. cinerea. (C) Comparison of VVLYK6 expression on grapevine berries infected with B. cinerea at two developmental stages, corresponding to berries at the veraison stage and ripe berries, respectively. For each bar plot, values represent the mean \pm SEM from three biologically independent experiments, and statistically significant groups are indicated by different letters (Kruskal–Wallis/BH posttest; p < 0.05). All transcriptomic data were generated from Kelloniemi et al. (2015).

Results

Analysis of VvLYK6 expression suggests an important role during *B. cinerea* infection

To investigate the role of VvLYK6 in grapevine immunity, we examined its expression profile using our previously published

transcriptomic dataset (Kelloniemi et al., 2015). Our analysis revealed that *VvLYK6* is upregulated in susceptible *V. vinifera* leaves at 24 and 48 h postinfection (hpi) with *B. cinerea*, whereas its expression remains unchanged following infection with *P. viticola* (Figure 1A). Given that VvLYK6 belongs to the LysM-RLK family known to perceive COS, these results are consistent with the presence of chitin in the fungal cell wall of *B. cinerea*, which

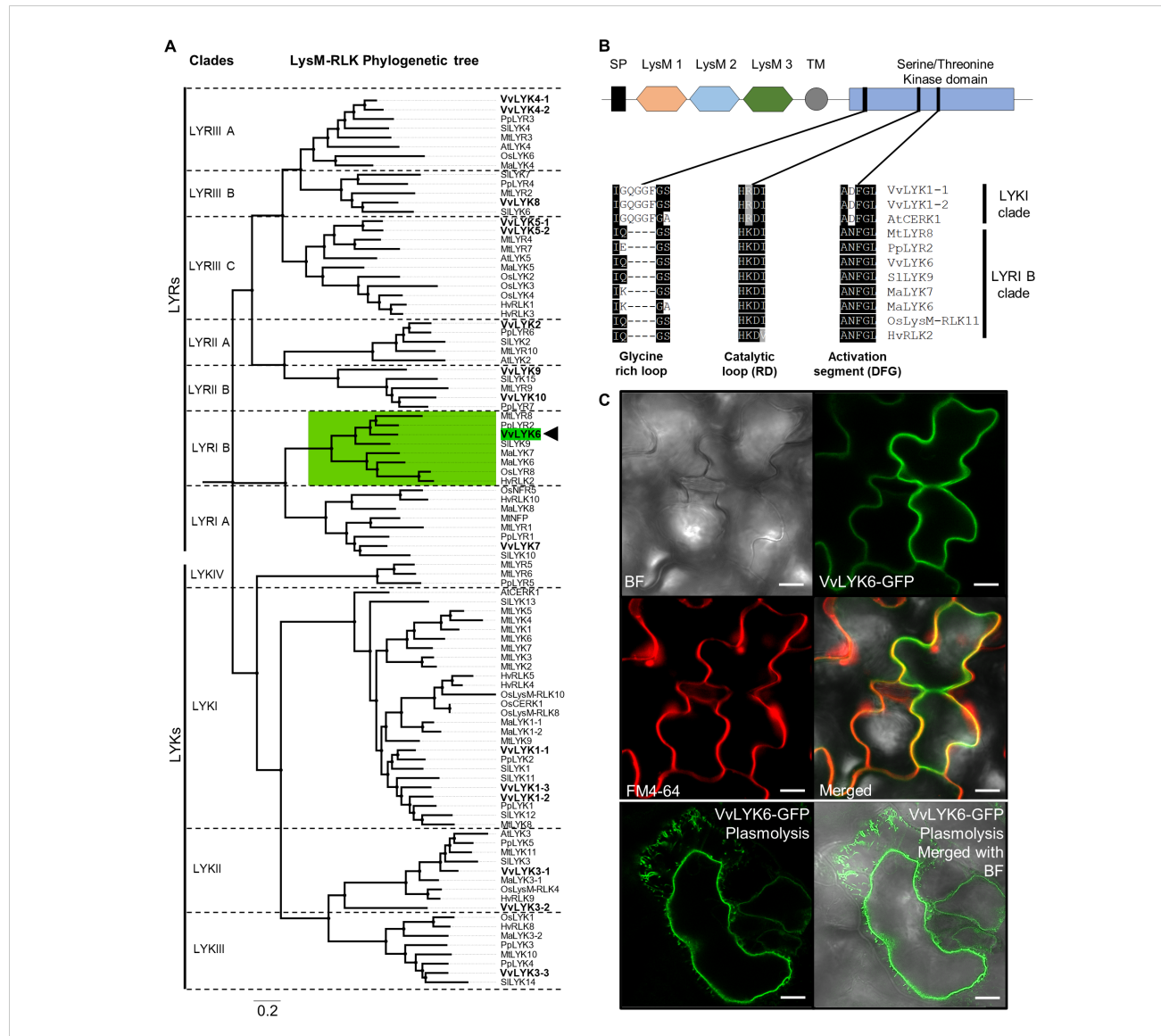


FIGURE 2

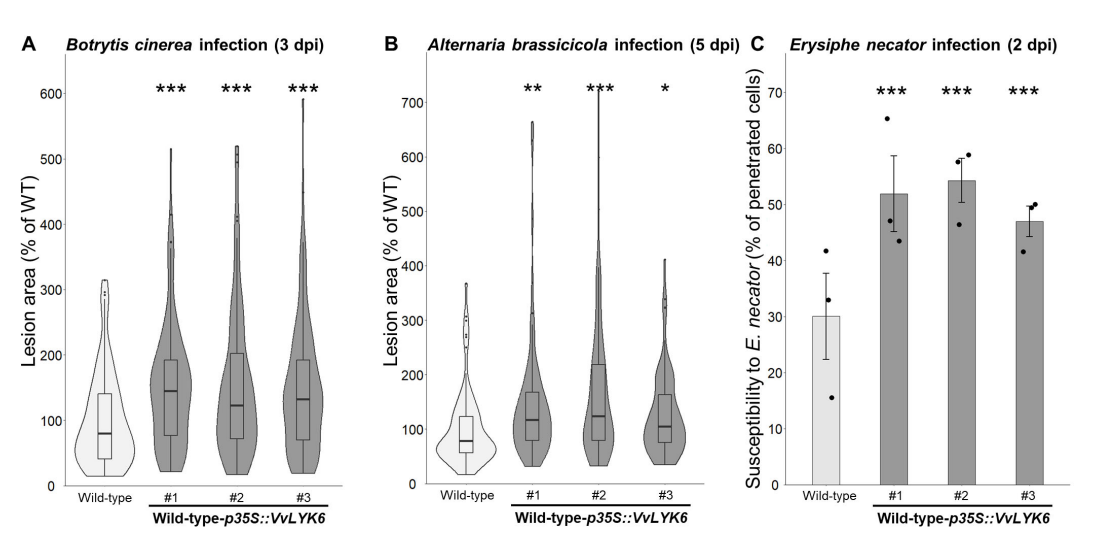
VvLYK6 belongs to the LYRI B phylogenetic clade of the LysM receptor-like kinases family. (A) A 1,000-bootstrap maximum-likelihood phylogenetic tree (Jones–Taylor–Thornton [JTT] model) including LysM-RLKs from eight plant species was constructed with MEGA X (Kumar et al., 2018). The phylogenetic tree was subdivided into clades according to the classification by Buendia et al. (2018). LYKs correspond to LysM-RLKs with an active kinase domain, whereas LYRs correspond to LYK-related LysM-RLKs lacking kinase activity. Protein sequences are listed in Supplementary Table S1. The 16 LysM-RLKs identified in the grapevine genome (VvLYKs) are shown in bold. VvLYK6 is highlighted in green and indicated by a black arrow within the green-surrounded LYRI B clade. (B) Schematic representation of putative VvLYK6 domains. Black square: signal peptide, hexagon: LysM domain (LysM1, orange; LysM2, blue; LysM3, green); grey circle: transmembrane domain; and blue square: kinase domain. Below the schematic VvLYK6 structure, alignments of motifs involved in kinase activity (glycine-rich loop, catalytic loop [RD], and activation segment [DFG motif]) are shown. Protein domain sequences were aligned with Clustal, performed on MEGAX (Kumar et al., 2018). Black and grey shading represent amino acid conservation. The alignment includes VvLYK1-1, VvLYK1-2, and AtCERK1 (LYKI clade), as well as MtLYR8, PpLYR2, VvLYK6, SlLYK9, MaLYK7, MaLYK6, OsLysM-RLK11/OsLYR8, and HvRLK2 (LYRI B clade). (C) Subcellular localization of VvLYK6 in A. thaliana leaves. GFP-tagged VvLYK6 in leaf segments of A. thaliana co-localizes with the plasma membrane marker probe (FM4-64). Plasmolysis of plant cells expressing VvLYK6 tagged with GFP reveals that the GFP signal does not localize to the cell wall. Scale bars represent 20 μm. Similar localization was observed in three independent lines. BF, Brightfield.

is nearly absent in that of the oomycete P. viticola. However, VvLYK6 expression was not significantly induced in grapevine cells treated with chitin hexamers (Supplementary Figure S2A). We also observed that *VvLYK6* expression is induced after 48 h of *B*. cinerea infection on grapevine fruits (Figure 1B) and particularly in infected mature berries (Figure 1C), which are known to be very susceptible to grey mold (Kelloniemi et al., 2015). To corroborate these results and confirm the upregulation of VvLYK6 during B. cinerea infection, we analyzed other publicly available transcriptomic data (Supplementary Figures S2B, C). In a first study on mature berries of the susceptible V. vinifera cv. Garganega inoculated or not with B. cinerea, VvLYK6 expression was significantly increased in infected berries compared to uninfected ones 12 days postinoculation (Lovato et al., 2019; Supplementary Figure S2B). In a second study comparing ripe berries of the susceptible V. vinifera cv. Pinot Noir with and without visible symptoms of B. cinerea infection (referred to as egression and pre-egression, respectively), the expression of VvLYK6 was significantly upregulated only in berries displaying visible symptoms (Haile et al., 2020; Supplementary Figure S2C). Altogether, these results showed a correlation between VvLYK6 upregulation in mature grapevine berries and their high susceptibility to B. cinerea.

VvLYK6 belongs to the LYRI B clade with a conserved domain of LysM-receptor-like kinase

To investigate the function of VvLYK6, we first conducted a phylogenetic analysis involving several plant species known to possess well-characterized LysM-RLKs associated with immunity and/or symbiosis. LysM-RLK protein sequences were retrieved from A. thaliana, Hordeum vulgare, Oryza sativa, Medicago truncatula, Musa acuminata, Prunus persica, Solanum lycopersicum, and V. vinifera (Supplementary Table S1). A total of 96 protein sequences were selected to construct a maximumlikelihood phylogenetic tree (Figure 2A). The resulting tree displays the two well-known subgroups (LYKs and LYRs), further divided into 11 clades as described by Buendia et al. (2018). The 16 members of the LysM-RLK family in V. vinifera are distributed across all clades except for the LYKIV clade, which is not conserved among dicots (Figure 2A). Our study focused on VvLYK6 (indicated by a black arrow), which belongs to the LYRI B clade, a group whose function has never been characterized in V. vinifera.

We began by analyzing the putative structure of VvLYK6, confirming the presence of all conserved domains typical of LysM-RLKs: a signal peptide, three extracellular LysM domains, a



Constitutive expression of VLYK6 in A. thaliana increases its susceptibility to different fungal pathogens. (A) Disease lesions percentages induced by B. cinerea on wild-type (WT) and the three independent transgenic lines expressing VLYK6, measured 3 days postinoculation; the lesion area on WT plants is referred to as 100%. A violin plot with an included box plot illustrates the distribution of lesion percentages of three independent experiments. For each biological replicate, 32 lesions were scored from eight plants per line, combining data from three biological replicates. Each transgenic line was statistically compared to the WT with the nonparametric Wilcoxon test (***p < 0.001). (B) Lesion percentages provoked by the necrotrophic fungus A. brassicicola on the WT and the three independent transgenic lines constitutively expressing VLYK6, measured 5 days postinoculation. A violin plot with an included box plot represents the distribution of lesion percentages in five independent experiments. For each biological replicate, 18 lesions were scored from four plants per line, combining data from four biological replicates. Each transgenic line was statistically compared to the WT using the nonparametric Wilcoxon test (***p < 0.001; *p < 0.05). (C) Penetration of the nonadapted powdery mildew E. p < 0.05 (C) Penetration of the nonadapted postinoculation. Bars represent the mean percentage of epidermal penetrated cells from three biologically independent experiments, each with more than 100 germinated conidia counted p < 0.001. ESM. Each transgenic line was statistically compared to the WT with a pairwise comparison of proportions test (***p < 0.001).

transmembrane domain, and a cytoplasmic putative serine/ threonine kinase domain (Figure 2B; Supplementary Table S3). Regarding the intracellular kinase domain, most of the amino acids of the kinase domain present in LYKI members (e.g., AtCERK1, VvLYK1-1, VvLYK1-2) were conserved in LYRI B orthologs, including VvLYK6 (Figure 2B). However, deletions observed in the glycine-rich loop, along with the lack of conservation in the catalytic loop and activation segment (both essential for kinase activity), suggest that the kinase domain of VvLYK6, as well as other members of the LYRI B, may be catalytically inactive (Hanks et al.,

1988; Klaus-Heisen et al., 2011). Specifically, while the glycine-rich loop typically contains three to four conserved glycine residues in most LYK subgroup members with kinase activity, only a single glycine residue is present in LYRI B members. Furthermore, other key motifs associated with kinase function, such as the catalytic loop (RD) and the activation segment (DFG), which are well conserved in active LYK kinases, are absent in the LYRI B clade (Figure 2B).

To determine the subcellular localization of VvLYK6, we expressed a C-terminal GFP-tagged version of the protein in *A. thaliana* and *V. vinifera*. Transgenic lines exhibited green

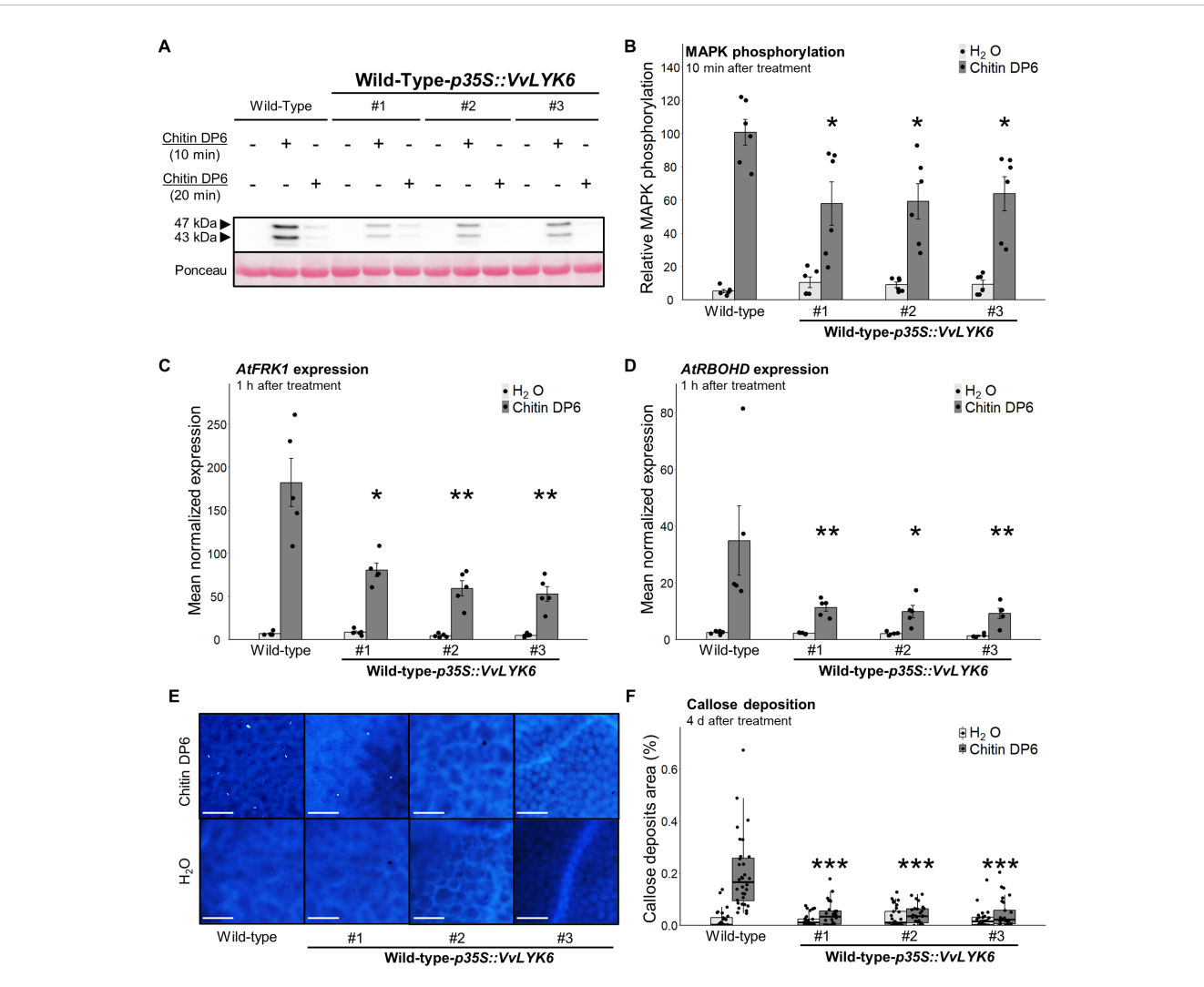
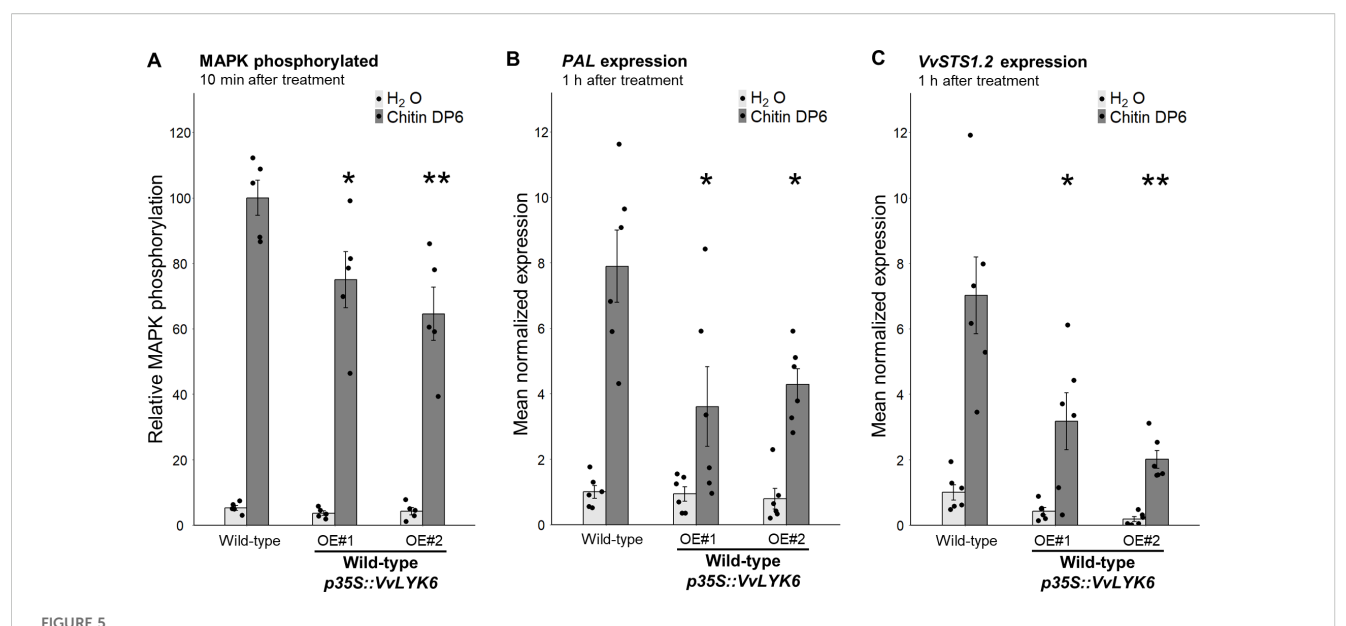


FIGURE 4
Constitutive expression of VVLYK6 inhibits chitin-triggered immune responses in *A. thaliana*. (**A, B**) MAPK phosphorylation was detected 10 or 20 min after H_2O (–) or chitin DP6 treatment (0.05 g/L) by immunoblotting with an antibody α -pERK1/2 in the wild-type (WT) and three independent lines constitutively expressing VvLYK6. (**A**) Representative immunoblotting with α -pERK1/2 and homogeneous loading verified by Ponceau red staining. (**B**) Quantification of the MAPKs phosphorylation at 10 min after treatment, detected by ImageQuant. Bars represent the mean \pm SEM on six biologically independent experiments. Each VvLYK6-expressing line treated with chitin DP6 was statistically compared to the WT with the nonparametric Wilcoxon test (*p < 0.05). (**C**, **D**) Normalized expression levels of AtFRK1 and AtRBOHD measured by qPCR 1 h after chitin DP6 (0.05 g/L) or H_2O treatment. The expression levels of AtFRK1 and AtRBOHD were normalized to those of two housekeeping genes. Bars represent the mean of relative expression \pm SEM of five biologically independent experiments. Asterisks indicate a statistically significant difference between each transgenic line and the WT treated with chitin DP6 (nonparametric Wilcoxon test; *p < 0.05); *p < 0.01). (**E**) Representative pictures of callose deposition after chitin DP6 (0.05 g/L) or H_2O treatment in WT and the three VvLYK6-expressing lines, observed 4 days posttreatment and analyzed by epifluorescence microscopy after aniline blue staining. Callose deposits were quantified using the Trainable Weka Segmentation plugin in ImageJ. (**F**) The box plot represents the distribution of the percentage of callose deposits on the total leaf surface for each genotype and condition, on at least 30 pictures per condition from three biologically independent experiments. Asterisks indicate statistically significant differences between each VvLYK6-expressing line and the WT treated with DP6 (Wilcoxon test, ***p < 0.001).



fluorescence from VvLYK6-GFP, which co-localized with the red fluorescence of the plasma membrane marker FM4-64 (Brandizzi et al., 2004) in both plant species (Figure 2C; Supplementary Figure S3). Plasmolysis experiments further confirmed that VvLYK6 followed the plasma membrane during cell shrinkage (Figure 2C), supporting its predicted localization at the plasma membrane.

Constitutive expression of VvLYK6 in *A. thaliana* increases its susceptibility to *B. cinerea* and other adapted or nonadapted fungal pathogens

To investigate the role of VvLYK6 during *B. cinerea* infection, and taking advantage of the fact that *VvLYK6* has no ortholog in *A. thaliana*, we constitutively expressed its gene from the susceptible *V. vinifera* cv. Marselan under the control of the *CaMV35S* promoter (*p35S*) in the WT ecotype Col-0 of *A. thaliana*. Three independent lines exhibiting high levels of *VvLYK6* transcripts were selected (Supplementary Figure S4A). To assess the impact of *VvLYK6* expression during fungal infections, leaves were inoculated with *B. cinerea*, and lesion areas were quantified 3 days postinoculation (dpi). As shown in Figure 3A; Supplementary Figure S4B, all three transgenic lines displayed a significant increase in susceptibility to *B. cinerea*, with lesion areas approximately 50% larger than those observed in WT plants.

We next examined whether VvLYK6 expression influenced susceptibility to other fungal pathogens. First, we tested the necrotrophic fungus *Alternaria brassicicola*, which is adapted to

Brassicaceae. At 5 dpi, the three transgenic lines showed significantly larger lesion areas, ranging from 26% to 67%, compared to WT plants (Figure 3B; Supplementary Figure S4C).

Finally, we evaluated the response to the nonadapted biotrophic fungus *Erysiphe necator* (grapevine powdery mildew). The Arabidopsis transgenic lines expressing *VvLYK6* exhibited a significantly higher rate of epidermal cell penetration compared to WT plants, with approximately 50% of cells penetrated in transgenic lines versus 30% in controls (Figure 3C).

All these results suggest that VvLYK6 may interfere with plant immune responses, thereby facilitating fungal colonization and spread.

Constitutive expression of VvLYK6 inhibits chitin-triggered immune responses in A. thaliana

To further elucidate the function of VvLYK6, we investigated early defense responses triggered by chitin by analyzing MAPK phosphorylation levels. As previously reported (Roudaire et al., 2023), chitin oligomers induce transient phosphorylation of two MAPKs of 43 and 47 kDa in *A. thaliana* WT plants (Figure 4A), corresponding to MPK3 and MPK6, respectively (Claverie et al., 2018). Interestingly, phosphorylation of both MAPKs, measured 10 min after treatment with chitin hexamers (DP6), was significantly reduced, by approximately 40%, in all three independent *VvLYK6*-expressing lines compared to WT plants (Figures 4A, B). To rule out a delayed activation of MAPKs

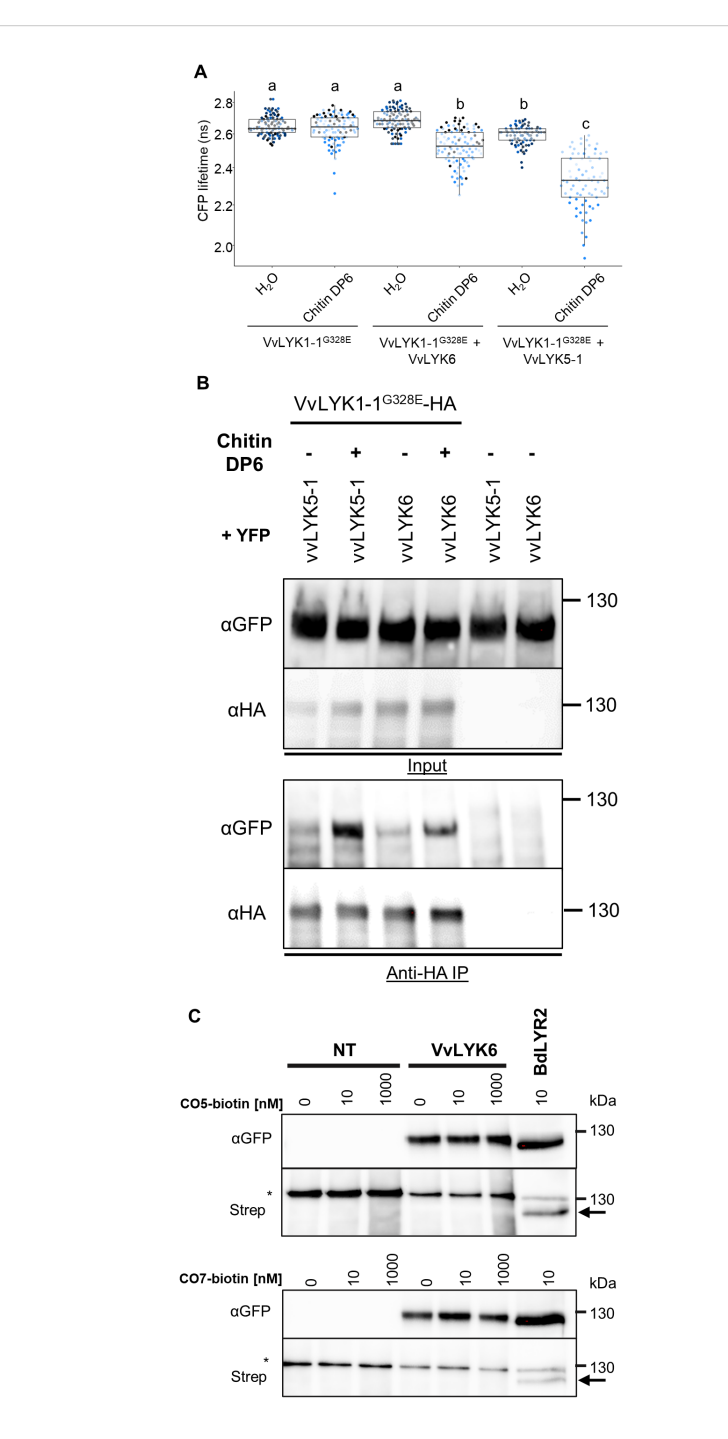


FIGURE 6

VvLYK6 interacts with VvLYK1-1 in the presence of chitin oligomers. (A) The dead kinase VvLYK1- 1^{G328E} -CFP was transiently expressed in *Nicotiana benthamiana* leaves, either alone or together with VvLYK6-YFP or VvLYK5-1-YFP, a protein known to interact with VvLYK1-1 in the presence of chitin DP6 (Roudaire et al., 2023). CFP lifetime (ns) was measured after leaf treatment with either water (H₂O) or chitin DP6 (0.1 g/L). Box plots represent the distribution of the data acquired from at least three biologically independent experiments. Different letters indicate a significant difference using a nonparametric Kruskal–Wallis test. (B) Co-immunopurification (Co-IP) of VvLYK1- 1^{G328E} -HA with VvLYK5-1:YFP and VvLYK6:YFP in the presence or absence of chitin DP6. Extracted proteins from *N. benthamiana* leaves were purified using anti-HA beads (anti-HA IP). After IP, the corresponding proteins were detected with anti-GFP antibodies (α -GFP) and anti-HA antibodies (α -HA). (C) The LysM-RLK VvLYK6 alone is not able to bind CO5 or CO7 with high affinity. VvLYK6-YFP and BdLYR2-YFP were transiently expressed in *N. benthamiana* leaves. Subsequently, microsomal fractions were prepared, and binding assays were conducted using a range of CO5-biotin or CO7-biotin as ligands. Microsomal fractions from leaves expressing BdLYR2-YFP were used as a positive control (black arrow), while those from nontransformed (NT) leaves served as a negative control. Western blotting was conducted using α -GFP and streptavidin-HRP. The quantities of microsomal fractions used correspond to 50 µg of total proteins for VvLYK6-YFP and NT, and 5 µg for BdLYR2-YFP. The asterisk indicates a nonspecific band (endogenously biotinylated protein) observed at 130 kDa. No binding with CO5- or CO7-biotin was observed for VvLYK6.

in transgenic lines, phosphorylation levels were also assessed 20 min posttreatment, but no compensatory increase was observed (Figure 4A).

In addition, we examined the expression of two defense-related genes: flagellin-induced receptor kinase 1 (*AtFRK1*) and respiratory burst oxidase homolog D (*AtRBOHD*), both known to be induced by chitin DP6 treatment (Morales et al., 2016; Brulé et al., 2019). Expression of *AtFRK1* was significantly reduced in the three transgenic lines, with transcript levels decreased by 56% to 71% compared to WT (Figure 4C). Similarly, *AtRBOHD* transcript levels were reduced by 67% to 74% in the *VvLYK6*-expressing lines (Figure 4D). To further explore the function of VvLYK6, we analyzed additional immune-related genes involved in hormonal signaling pathways, such as salicylic acid (SA) and jasmonic acid (JA) (Spoel et al., 2003). No significant differences were observed in the expression of the SA- and JA-responsive genes *PR1* and *PDF1.2* between the three independent *VvLYK6*-expressing lines and WT plants following chitin DP6 treatment (Supplementary Figure S5).

We then examined the impact of VvLYK6 expression on callose deposition, a later-stage defense response. Chitin is well known to induce callose accumulation in *A. thaliana* leaves (Roudaire et al., 2023). Compared to WT plants, all transgenic lines expressing *VvLYK6* exhibited a significantly reduced percentage of callose deposits four days after chitin DP6 treatment (Figures 4E, F). Specifically, WT leaves showed callose deposits covering 0.2% of the total leaf area, whereas the transgenic lines averaged only 0.04%, a level comparable to water-treated controls (Figures 4E, F).

Taken together, these results clearly indicate that VvLYK6 expression in *A. thaliana* suppresses chitin-triggered immune responses.

Although our study primarily focused on the role of VvLYK6 during fungal infection and chitin perception, given its induction during *B. cinerea* infection, we also tested its specificity by analyzing responses to a bacterial MAMP: the flagellin-derived peptide flg22 (Trdá et al., 2014). MAPK phosphorylation was assessed 10 min after flg22 treatment in WT and *VvLYK6*-expressing lines. Immunoblot analysis revealed no significant differences between the transgenic lines and WT (Supplementary Figure S6A). As flg22 is also known to inhibit plant growth in *A. thaliana* (Vetter et al., 2012), flg22-induced growth inhibition assays were performed. After 12 days of growth on a medium containing 1 μM flg22, no significant differences in growth inhibition were observed between WT and *VvLYK6*-expressing seedlings (Supplementary Figure S6B).

These findings demonstrate that VvLYK6 expression in *A. thaliana* does not interfere with flg22-triggered immune signaling but appears to specifically modulate chitin-induced immune responses associated with fungal pathogens.

VvLYK6 represses chitin-triggered immunity in grapevine (Vitis vinifera)

To validate the findings observed in *A. thaliana*, we investigated the function of VvLYK6 in *V. vinifera*. Two independent grapevine cell lines constitutively expressing VvLYK6 tagged with GFP and exhibiting high transcript and protein levels were selected (Supplementary Figures S7A, B).

Chitin oligomers are known to elicit phosphorylation of two MAPKs (45 and 49 kDa) in grapevine cells (Brulé et al., 2019). Compared to WT cells, MAPK phosphorylation induced by chitin DP6 was significantly reduced by 25% to 35% in both transgenic lines (VvLYK6 OE#1 and OE#2) after 10 min of treatment (Figure 5A; Supplementary Figure S7C). We also quantified the expression of two defense-related genes involved in the stilbene biosynthetic pathway, which contributes to phytoalexin production in grapevine: VvPAL (phenylalanine ammonia lyase) and VvSTS1.2 (stilbene synthase). One hour after chitin DP6 treatment, the constitutive expression of VvLYK6 significantly impaired the induction of both genes. The typical upregulation of VvPAL and VvSTS1.2 was reduced by more than 50% in the transgenic lines compared to WT cells (Figures 5B, C). Overall, these results suggest that VvLYK6 acts as a negative regulator of chitin-triggered immune responses in V. vinifera, consistent with the observations made in A. thaliana.

VvLYK6 forms a receptor complex with VvLYK1-1 in the presence of chitin oligomers

During fungal infection or in the presence of chitin, VvLYK1-1 has been identified as a key co-receptor involved in chitin-triggered immune signaling in grapevine (Brulé et al., 2019). Notably, VvLYK1-1 is the only LysM-RLK shown to form a receptor complex with VvLYK5-1 to perceive chitin and activate downstream defense responses (Roudaire et al., 2023).

To explain the repression of MTI observed when VvLYK6 is overexpressed, we hypothesized a potential interaction between the functional co-receptor VvLYK1-1 and VvLYK6. To test this, we performed FRET-FLIM (Förster resonance energy transfer by fluorescence lifetime imaging) experiments following transient coexpression of both proteins fused to CFP and YFP, respectively. Since constitutive expression of VvLYK1-1 induces strong cell death in Nicotiana benthamiana, we used a kinase-dead version carrying the G328E mutation (VvLYK1-1^{G328E}-CFP). As expected, the CFP lifetime of VvLYK1-1^{G328E}-CFP expressed alone was unaffected by chitin treatment (Figure 6A). However, co-expression with VvLYK6-YFP followed by chitin DP6 treatment resulted in a significant decrease in CFP lifetime, indicating a ligand-dependent in vivo interaction between these two LysM-RLKs (Figure 6A). This interaction was further confirmed by co-immunoprecipitation (Co-IP) assays, which demonstrated that VvLYK6-YFP physically associates with VvLYK1-1^{G328E}-HA in the presence of chitin DP6 (Figure 6B). In both experiments, VvLYK5-1 was used as a positive control, as its interaction with VvLYK1-1 in a ligand-dependent manner has been previously described (Figures 6A, B; Roudaire et al., 2023). Interestingly, VvLYK6 and VvLYK1-1 primarily interact in the presence of chitin DP6, suggesting that VvLYK6 may possess affinity for chitin oligomers. Indeed, some LYRI B orthologs have been reported to bind both short- and long-chain chitin oligomers with high affinity (Li et al., 2022; Ding et al., 2025). To evaluate the binding capacity of VvLYK6, we used cross-linkable

biotinylated versions of chitin pentamer and heptamer (CO5- and CO7-biotin) to assess its interaction with chitin oligomers. Surprisingly, unlike its orthologs in *Brachypodium distachyon* (BdLYR2) and *Medicago truncatula* (MtLYR8), VvLYK6 did not exhibit high-affinity binding to either CO5 or CO7 (Figure 6C; Li et al., 2022; Ding et al., 2025). This discrepancy may be due to improper folding of VvLYK6 when overexpressed in *Nicotiana benthamiana* leaves, resulting in a nonfunctional protein. Alternatively, VvLYK6 may require association with VvLYK1-1 to properly bind chitin oligomers and initiate signal transduction. Supporting this latter hypothesis, constitutive expression of VvLYK6 in the *Arabidopsis* mutant *Atcerk1* failed to activate MAPK phosphorylation or induce *FRK1* expression following chitin DP6 treatment (Supplementary Figure S8). These findings

suggest that VvLYK6 may not function as a primary chitin receptor but could act as a modulator of immune signaling through interaction with VvLYK1-1.

Discussion

B. cinerea is among the most devastating fungal pathogens affecting a wide range of plant species. This necrotrophic fungus is particularly known for infecting mature berries of susceptible V. vinifera cultivars, leading to significant reductions in yield and must quality during winemaking (Fillinger and Elad, 2016). Numerous transcriptomic studies have highlighted the upregulation of specific genes during berry ripening, a

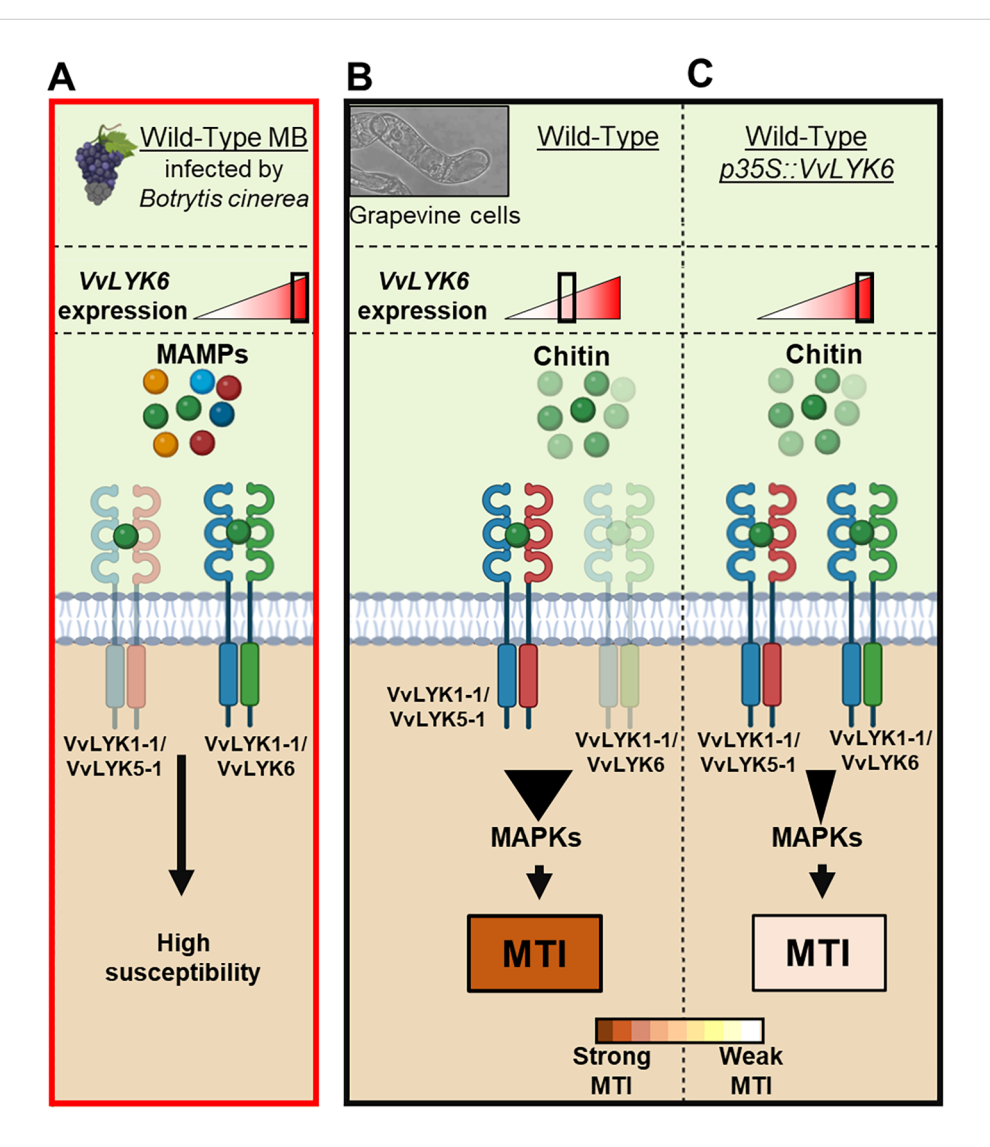


FIGURE 7

Proposed mode of action of VvLYK6 in modulating plant immune responses. VvLYK6 is involved in grapevine susceptibility during *Botrytis cinerea* infection and repression of chitin oligomer elicitation. (A) *VvLYK6* expression is induced during *Botrytis cinerea* infection in mature berries (MB), correlating with the absence of defense gene expression (*VvSTS1.2* and *VvPAL*) and a high susceptibility to fungal pathogens (Kelloniemi et al., 2015). (B) Formation of a VvLYK1-1/VvLYK5-1 complex after perception of chitin oligomers at the plasma membrane activates strong MAMP-triggered immunity (MTI) in grapevine cells (Roudaire et al., 2023). (C) Constitutive expression of VvLYK6, which interacts with VvLYK1-1, might deplete VvLYK1-1 available for interaction with VvLYK5-1 and thereby decrease chitin-triggered plant defense responses. Receptors are classified by color: blue, VvLYK1-1; red, VvLYK5-1; and green, VvLYK6.

developmental stage highly susceptible to infection (Kelloniemi et al., 2015; Lovato et al., 2019; Haile et al., 2020).

Chitin, a major structural component of fungal cell walls, is recognized as a MAMP. In the context of *B. cinerea* infection, we focused on the well-characterized LysM-RLK family, which plays a key role in the perception of chitin oligomers and the activation of immune responses. In susceptible *V. vinifera* varieties, *VvLYK6* has been identified as the most highly expressed LysM-RLK during *B. cinerea* infection in mature berries (Kelloniemi et al., 2015; Brulé et al., 2019), a finding further supported by additional transcriptomic analyses (Lovato et al., 2019; Haile et al., 2020).

Our study provides new insights into the role of *VvLYK6*, a member of the newly defined LYRI B subfamily. Unexpectedly, we found that the constitutive expression of *VvLYK6* in *A. thaliana* significantly increases the plant's susceptibility to *B. cinerea* and two other adapted and nonadapted fungal pathogens. More specifically, our results indicate that the inhibitory function of *VvLYK6* is confined to the chitin-triggered defense pathway associated with fungal pathogens.

In V. vinifera, the constitutive expression of VvLYK6 similarly inhibits the chitin-triggered immune pathway. Moreover, VvLYK6 has been shown to form a heterodimeric complex with VvLYK1-1 in the presence of chitin oligomers, suggesting potential competition between VvLYK6 and VvLYK5-1 for complex formation with VvLYK1-1 (Roudaire et al., 2023). During B. cinerea infection in mature berries, the upregulation of VvLYK6 may lead to a predominance of VvLYK1-1/VvLYK6 complexes, especially since VvLYK6 expression does not affect VvLYK5-1 transcript levels (Supplementary Figure S7D). This could negatively regulate the formation of VvLYK1-1/VvLYK5-1 complexes, supporting a model in which VvLYK6 expression modulates chitin-triggered immunity in grapevine (Figure 7). A similar regulatory mechanism has been described in rice within the LysM-RLK family. The rice ortholog of VvLYK1-1, OsCERK1, is known to participate in both immune responses via interaction with OsCEBIP and AM symbiosis via interaction with OsMYR1. Notably, constitutive expression of OsMYR1, a member of the LYRI A clade, significantly reduces disease resistance in rice (Zhang et al., 2021). This study indicates that OsMYR1 dampens defense signaling by preventing OsCERK1 from phosphorylating its substrates. A comparable mechanism might occur between VvLYK1-1 and VvLYK6 to block the activation of the defense signaling pathway in grapevine. Analogous regulatory dynamics have also been observed in other RLK families. For instance, the leucine-rich repeat RLK BIR2 acts as a negative regulator by forming a complex with ASSOCIATED RECEPTOR KINASE 1 (BAK1), thereby preventing BAK1 from associating with ligandbinding receptors, such as FLS2, in the presence of MAMPs (Halter et al., 2014).

During chitin-triggered immunity in *V. vinifera*, *VvLYK6* expression appears to be negatively correlated with the expression of the well-established defense-related genes *VvPAL* and *VvSTS1.2*, encoding the phenylalanine ammonia lyase and the stilbene synthase, respectively. These two enzymes catalyze the final step in the biosynthesis of resveratrol, the main grapevine phytoalexin.

When VvLYK6 is overexpressed in grapevine cells, the expression of VvPAL and VvSTS1.2 is significantly suppressed. These findings are consistent with the observed susceptibility of V. vinifera to B. cinerea during berry ripening. While green berries typically exhibit basal resistance to B. cinerea, mature berries become highly susceptible at harvest. At the veraison stage, Kelloniemi et al. (2015) showed that the defense-related genes VvPAL and VvSTS1.2 are significantly upregulated in green berries infected by B. cinerea, leading to the accumulation of resveratrol, while the expression of VvLYK6 remains very low. In contrast, in mature berries, VvLYK6 is strongly upregulated during infection, while VvPAL and VvSTS1.2 are not induced, resulting in increased susceptibility to the pathogen (Kelloniemi et al., 2015). Our findings suggest that VvLYK6 may act as a key molecular component influencing the expression of VvPAL and VvSTS1.2, thereby modulating grapevine susceptibility to *B. cinerea* infection. Interestingly, similar patterns have been observed in other species, such as tomato, where ripe fruits are significantly more susceptible to B. cinerea than unripe ones (Silva et al., 2021). In that study, transcriptomic analyses revealed an upregulation of SILYK9, the tomato ortholog of VvLYK6 (Figure 1), in ripe fruits infected by the necrotrophic fungi B. cinerea and Rhizopus stolonifer (Supplementary Figure S9). As in grapevine, the upregulation of SlLYK9 correlates with increased susceptibility in mature tomato fruits, suggesting a conserved role in the suppression of plant defense responses (Silva et al., 2021). These observations point to a broader functional role for LysM-RLKs belonging to the LYRI B clade. While LYRI B members have traditionally been associated with the establishment of symbiosis (Li et al., 2022; Ding et al., 2025), emerging evidence suggests that they may also act as negative regulators of plant immunity across different organs and plantfungus interactions. This dual role is supported by their expression in both root and aerial tissues (leaves and fruits) in grapevine and tomato (Supplementary Figure S10) (Zouine et al., 2017). Such functional versatility has also been reported for other LysM-RLK clades. Members of the LYRI A clade, for example, are involved in symbiosis and can act as either positive or negative regulators of immunity, depending on the plant species (Buendia et al., 2018; Zhang et al., 2021), although their expression is typically restricted to roots. Similarly, LYRIII C genes function as negative regulators of both immunity and AM symbiosis and are expressed in both root and aerial tissues (Wang et al., 2023). Taken together, these findings suggest that LYRI B members may serve as repressors of plant immunity in aerial organs during B. cinerea infection, while also contributing to AM symbiosis in roots. The potential role of VvLYK6 in AM establishment warrants further investigation, particularly since, unlike other LYRI B proteins, it does not appear to retain a high affinity for COS.

From an evolutionary perspective, we analyzed the LYK6 receptor sequence from *Muscadinia rotundifolia* (MrLYK6), a species closely related to *V. vinifera* and naturally resistant to *B. cinerea* (Gabler et al., 2003). Sequence alignment between MrLYK6 and VvLYK6 revealed a high identity of 95.4%, with more than half of the amino acid variations located within the LysM2 domain (Supplementary Figure S11A). This domain has

been shown to play a critical role in chitin binding in OsCEBIP, AtCERK1, and OsCERK1, with specific residues directly involved in ligand interaction (Liu et al., 2012; Hayafune et al., 2014; Xu et al., 2023). Notably, multiple sequence alignment revealed differences between VvLYK6 and MrLYK6 at several key residues known to be essential for chitin binding in the aforementioned receptors (Supplementary Figures S11A, B). To further investigate these differences, we used AlphaFold3 to predict the three-dimensional structures of the LysM2 domains of VvLYK6 and MrLYK6, based on the crystallized structure of OsCERK1 bound to a chitin hexamer (Xu et al., 2023). These structural models revealed distinct differences in both electrostatic charge distribution and conformational features within the chitin-binding region (Supplementary Figure S11C). Taken together, these natural variations in the LysM2 domain of VvLYK6 may explain its lack of detectable affinity for chitin oligomers when expressed alone (Figure 6C). Conversely, the putative chitin-binding capacity of MrLYK6 could contribute to the enhanced resistance of M. rotundifolia to B. cinerea, highlighting the evolutionary divergence of LysM-RLK function even among closely related species.

To conclude, our study demonstrates that VvLYK6 forms a chitin-induced receptor complex with VvLYK1-1 and that its overexpression negatively regulates plant immune responses, thereby enhancing susceptibility to *B. cinerea* and other fungal pathogens. These findings support the classification of *VvLYK6*, particularly in susceptible *V. vinifera* cultivars, as a susceptibility (*S*) gene (Zaidi et al., 2018). Consequently, targeted knockout of *VvLYK6* represents a promising strategy to improve grapevine resistance to *B. cinerea* and potentially other fungal pathogens. In line with the growing interest in *S* genes as complementary or alternative targets to classical resistance (*R*) genes in crop improvement, *VvLYK6* emerges as a compelling candidate for genome editing approaches.

Data availability statement

Publicly available datasets were analyzed in this study. This data can be found here: Kelloniemi J, Trouvelot S, Héloir M-C, Simon A, Dalmais B, Frettinger P, Cimerman A, Fermaud M, Roudet J, Baulande S, et al. (2015) Analysis of the molecular dialogue between gray mold (*Botrytis cinerea*) and grapevine (*Vitis vinifera*) reveals a clear shift in defense mechanisms during berry ripening. MPMI 28: 1167–1180 Lovato A, Zenoni S, Tornielli GB, Colombo T, Vandelle E, Polverari A (2019) Plant and fungus transcriptomic data from grapevine berries undergoing artificially-induced noble rot caused by *Botrytis cinerea*. Data in Brief 25: 104150 Haile ZM, Malacarne G, Pilati S, Sonego P, Moretto M, Masuero D, Vrhovsek U, Engelen K, Baraldi E, Moser C (2020) Dual transcriptome and metabolic analysis of *Vitis vinifera* cv. Pinot Noir berry and *Botrytis cinerea* during quiescence and egressed infection. Front Plant Sci 10: 1704.

Author contributions

JV: Conceptualization, Data curation, Formal Analysis, Investigation, Methodology, Supervision, Visualization, Writing – original draft, Writing – review & editing. TM: Investigation, Validation, Writing – original draft, Writing – review & editing. DL: Investigation, Methodology, Validation, Writing – original draft, Writing – review & editing. TR: Investigation. AK: Methodology, Writing – original draft. NL-C: Methodology, Writing – review & editing. CV: Investigation, Methodology, Writing – original draft. VG: Investigation, Methodology, Writing – original draft. CP: Investigation, Methodology, Writing – original draft. BL: Supervision, Writing – original draft, Writing – review & editing. M-CH: Supervision, Writing – original draft, Writing – review & editing. BP: Conceptualization, Funding acquisition, Project administration, Supervision, Resources, Writing – original draft, Writing – review & editing.

Funding

The author(s) declare that financial support was received for the research and/or publication of this article. This work was supported by the Plant2Pro[®] Carnot Institute as part of its 2020 call for projects (VitiLYKs project, Grant No. C4520), which is funded by the French National Research Agency (ANR 20-CARN-024-01) and the PPR VITAE program (ANR 20-PCPA-0010).

Acknowledgments

We acknowledge Abdelwahad Echairi and Anna Beslic (SATT Sayens, Dijon, France) for providing the *E. necator* strain. We also acknowledge Dr. Christian Steinberg for the *A. brassicicola* inoculum strain MIAE01824, originating from the Agroecology unit collection (UMR1347, Dijon, France). We thank Cécile Blanchard for her technical support with infections involving the different pathogens. We also thank Elodie Noirot for confocal microscopy support from the regional Centre of Microscopy/DImaCell platform (Dijon, France). Finally, we acknowledge the France-BioImaging infrastructure supported by the French National Research Agency (ANR-10-INBS-04).

Conflict of interest

The authors declare that the research was conducted in the absence of any commercial or financial relationships that could be construed as a potential conflict of interest.

Generative Al statement

The author(s) declare that no Generative AI was used in the creation of this manuscript.

Any alternative text (alt text) provided alongside figures in this article has been generated by Frontiers with the support of artificial intelligence and reasonable efforts have been made to ensure accuracy, including review by the authors wherever possible. If you identify any issues, please contact us.

Publisher's note

All claims expressed in this article are solely those of the authors and do not necessarily represent those of their affiliated organizations, or those of the publisher, the editors and the reviewers. Any product that may be evaluated in this article, or claim that may be made by its manufacturer, is not guaranteed or endorsed by the publisher.

Supplementary material

The Supplementary Material for this article can be found online at: https://www.frontiersin.org/articles/10.3389/fpls.2025.1705961/full#supplementary-material

References

Adrian, M., Corio-Costet, M.-F., Calonnec, A., Cluzet, S., Poinssot, B., Trouvelot, S., et al. (2024). "Chapter Four - Grapevine defence mechanisms when challenged by pathogenic fungi and oomycetes," in *Advances in Botanical Research. Grapevine: From Origin to the Vineyard.* Ed. P. Martins-Lopes (San Diego, CA: Academic Press), 101–195

Ahuja, I., Kissen, R., and Bones, A. M. (2012). Phytoalexins in defense against pathogens. *Trends Plant Sci* 17, 73–90. doi: 10.1016/j.tplants.2011.11.002

Ao, Y., Li, Z., Feng, D., Xiong, F., Liu, J., Li, J., et al. (2014). OsCERK 1 and OsRLCK 176 play important roles in peptidoglycan and chitin signaling in rice innate immunity. *Plant J.* 80, 1072–1084. doi: 10.1111/tpj.12710

Böhm, H., Albert, I., Oome, S., Raaymakers, T. M., Van Den Ackerveken, G., and Nürnberger, T. (2014). A conserved peptide pattern from a widespread microbial virulence factor triggers pattern-induced immunity in Arabidopsis. *PloS Pathog.* 10, e1004491. doi: 10.1371/journal.ppat.1004491

Boller, T., and Felix, G. (2009). A renaissance of elicitors: Perception of microbe-associated molecular patterns and danger signals by pattern-recognition receptors. *Annu. Rev. Plant Biol.* 60, 379–406. doi: 10.1146/annurev.arplant.57.032905.105346

Brandizzi, F., Irons, S. L., Johansen, J., Kotzer, A., and Neumann, U. (2004). GFP is the way to glow: bioimaging of the plant endomembrane system. *J. Microscopy* 214, 138–158. doi: 10.1111/j.0022-2720.2004.01334.x

Brulé, D., Villano, C., Davies, L. J., Trdá, L., Claverie, J., Héloir, M., et al. (2019). The grapevine (*Vitis vinifera*) LysM receptor kinases Vv LYK 1-1 and Vv LYK 1-2 mediate chitooligosaccharide-triggered immunity. *Plant Biotechnol. J.* 17, 812–825. doi: 10.1111/pbi.13017

Buendia, L., Girardin, A., Wang, T., Cottret, L., and Lefebvre, B. (2018). LysM Receptor-Like Kinase and LysM Receptor-Like Protein families: An update on phylogeny and functional characterization. *Front. Plant Sci.* 9, 1531. doi: 10.3389/fpls.2018.01531

Buendia, L., Wang, T., Girardin, A., and Lefebvre, B. (2016). The LysM receptor-like kinase SlLYK10 regulates the arbuscular mycorrhizal symbiosis in tomato. *New Phytol.* 210, 184–195. doi: 10.1111/nph.13753

Cao, Y., Liang, Y., Tanaka, K., Nguyen, C. T., Jedrzejczak, R. P., Joachimiak, A., et al. (2014). The kinase LYK5 is a major chitin receptor in Arabidopsis and forms a chitin-induced complex with related kinase CERK1. *eLife* 3, e03766. doi: 10.7554/eLife.03766.024

Claverie, J., Balacey, S., Lemaître-Guillier, C., Brulé, D., Chiltz, A., Granet, L., et al. (2018). The cell wall-derived xyloglucan is a new DAMP triggering plant immunity in *Vitis vinifera* and *Arabidopsis thaliana*. *Front. Plant Sci.* 9, 1725. doi: 10.3389/fpls.2018.01725

Clough, S. J., and Bent, A. F. (1998). Floral dip: a simplified method for *Agrobacterium*-mediated transformation of *Arabidopsis thaliana*. *Plant J.* 16, 735–743. doi: 10.1046/j.1365-313x.1998.00343.x

Cullimore, J., Fliegmann, J., Gasciolli, V., Gibelin-Viala, C., Carles, N., Luu, T.-B., et al. (2023). Evolution of lipochitooligosaccharide binding to a LysM-RLK for nodulation in *Medicago truncatula*. *Plant And Cell Physiol*. 64, 746–757. doi: 10.1093/pcp/pcad033

Ding, Y., Lesterps, Z., Gasciolli, V., Fuchs, A. L., Gaston, M., Medioni, L., et al. (2025). Several groups of LysM-RLKs are involved in symbiotic signal perception and arbuscular mycorrhiza establishment. *Nat. Commun.* 16, 5999. doi: 10.1038/s41467-025-60717-1

Ding, Y., Wang, T., Gasciolli, V., Reyt, G., Remblière, C., Marcel, F., et al. (2024). The LysM Receptor-Like Kinase SlLYK10 controls lipochitooligosaccharide signaling in inner cell layers of tomato roots. *Plant Cell Physiol.* 65, 1149–1159. doi: 10.1093/pcp/pcae035

Feechan, A., Anderson, C., Torregrosa, L., Jermakow, A., Mestre, P., Wiedemann-Merdinoglu, S., et al. (2013). Genetic dissection of a TIR-NB-LRR locus from the wild North American grapevine species *Muscadinia rotundifolia* identifies paralogous genes conferring resistance to major fungal and oomycete pathogens in cultivated grapevine. *Plant J.* 76, 661–674. doi: 10.1111/tpj.12327

Feng, F., Sun, J., Radhakrishnan, G. V., Lee, T., Bozsóki, Z., Fort, S., et al. (2019). A combination of chitooligosaccharide and lipochitooligosaccharide recognition promotes arbuscular mycorrhizal associations in Medicago truncatula. *Nat. Commun.* 10, 5047. doi: 10.1038/s41467-019-12999-5

Fillinger, S., and Elad, Y. (2016). Botrytis – the Fungus, the Pathogen and its Management in Agricultural Systems. Botrytis – The Fungus, the Pathogen and its Management in Agricultural Systems. (Berlin: Springer International Publishing). doi: 10.1007/978-3-319-23371-0

Gabler, F. M., Smilanick, J. L., Mansour, M., Ramming, D. W., and Mackey, B. E. (2003). Correlations of morphological, anatomical, and chemical features of grape berries with resistance to *Botrytis cinerea*. *Phytopathology*[®] 93, 1263–1273. doi: 10.1094/PHYTO.2003.93.10.1263

Gimenez-Ibanez, S., Hann, D. R., Ntoukakis, V., Petutschnig, E., Lipka, V., and Rathjen, J. P. (2009). AvrPtoB targets the LysM Receptor Kinase CERK1 to promote bacterial virulence on plants. *Curr. Biol.* 19, 423–429. doi: 10.1016/j.cub.2009.01.054

Girardin, A., Wang, T., Ding, Y., Keller, J., Buendia, L., Gaston, M., et al. (2019). LCO receptors involved in arbuscular mycorrhiza are functional for rhizobia perception in legumes. *Curr. Biol.* 29, 4249–4259.e5. doi: 10.1016/j.cub.2019.11.038

Haile, Z. M., Malacarne, G., Pilati, S., Sonego, P., Moretto, M., Masuero, D., et al. (2020). Dual transcriptome and metabolic analysis of *Vitis vinifera* cv. Pinot Noir berry and *Botrytis cinerea* during quiescence and egressed infection. *Front. Plant Sci.* 10, 1704. doi: 10.3389/fpls.2019.01704

Halter, T., Imkampe, J., Mazzotta, S., Wierzba, M., Postel, S., Bücherl, C., et al. (2014). The Leucine-Rich Repeat Receptor Kinase BIR2 is a negative regulator of BAK1 in plant immunity. *Curr. Biol.* 24, 134–143. doi: 10.1016/j.cub.2013.11.047

Hanks, S. K., Quinn, A. M., and Hunter, T. (1988). The protein kinase family: Conserved features and deduced phylogeny of the catalytic domains. *Science* 241, 42–52. doi: 10.1126/science.3291115

Hayafune, M., Berisio, R., Marchetti, R., Silipo, A., Kayama, M., Desaki, Y., et al. (2014). Chitin-induced activation of immune signaling by the rice receptor CEBiP relies on a unique sandwich-type dimerization. *Proc. Natl. Acad. Sci. U.S.A* 111, E404–E413. doi: 10.1073/pnas.1312099111

He, J., Zhang, C., Dai, H., Liu, H., Zhang, X., Yang, J., et al. (2019). A LysM receptor heteromer mediates perception of arbuscular mycorrhizal symbiotic signal in rice. *Mol. Plant* 12, 1561–1576. doi: 10.1016/j.molp.2019.10.015

Jones, D. T., Taylor, W. R., and Thornton, J. M. (1992). The rapid generation of mutation data matrices from protein sequences. *Bioinformatics* 8, 275–282. doi: 10.1093/bioinformatics/8.3.275

Karimi, M., De Meyer, B., and Hilson, P. (2005). Modular cloning in plant cells. Trends Plant Sci 10, 103–105. doi: 10.1016/j.tplants.2005.01.008

Kelloniemi, J., Trouvelot, S., Héloir, M.-C., Simon, A., Dalmais, B., Frettinger, P., et al. (2015). Analysis of the molecular dialogue between gray mold (*Botrytis cinerea*) and grapevine (*Vitis vinifera*) reveals a clear shift in defense mechanisms during berry ripening. *MPMI* 28, 1167–1180. doi: 10.1094/MPMI-02-15-0039-R

Klaus-Heisen, D., Nurisso, A., Pietraszewska-Bogiel, A., Mbengue, M., Camut, S., Timmers, T., et al. (2011). Structure-function similarities between a plant receptor-like kinase and the human interleukin-1 receptor-associated kinase-4. *J. Biol. Chem.* 286, 11202–11210. doi: 10.1074/jbc.M110.186171

Kumar, S., Stecher, G., Li, M., Knyaz, C., and Tamura, K. (2018). MEGA X: Molecular Evolutionary Genetics Analysis across computing platforms. *Mol. Biol. Evol.* 35, 1547–1549. doi: 10.1093/molbev/msy096

- Li, X.-R., Sun, J., Albinsky, D., Zarrabian, D., Hull, R., Lee, T., et al. (2022). Nutrient regulation of lipochitooligosaccharide recognition in plants *via* NSP1 and NSP2. *Nat. Commun.* 13, 6421. doi: 10.1038/s41467-022-33908-3
- Liu, T., Liu, Z., Song, C., Hu, Y., Han, Z., She, J., et al. (2012). Chitin-induced dimerization activates a plant immune receptor. *Science* 336, 1160–1164. doi: 10.1126/science.1218867
- Liu, H., and Naismith, J. H. (2008). An efficient one-step site-directed deletion, insertion, single and multiple-site plasmid mutagenesis protocol. *BMC Biotechnol.* 8, 91. doi: 10.1186/1472-6750-8-91
- Lovato, A., Zenoni, S., Tornielli, G. B., Colombo, T., Vandelle, E., and Polverari, A. (2019). Plant and fungus transcriptomic data from grapevine berries undergoing artificially-induced noble rot caused by *Botrytis cinerea*. *Data Brief* 25, 104150. doi: 10.1016/j.dib.2019.104150
- Mason, K. N., Ekanayake, G., and Heese, A. (2020). "Staining and automated image quantification of callose in Arabidopsis cotyledons and leaves," in *Methods in Cell Biology* (San Diego, CA: Elsevier), 181–199.
- Miya, A., Albert, P., Shinya, T., Desaki, Y., Ichimura, K., Shirasu, K., et al. (2007). CERK1, a LysM receptor kinase, is essential for chitin elicitor signaling in *Arabidopsis*. *Proc. Natl. Acad. Sci. U.S.A.* 104, 19613–19618. doi: 10.1073/pnas.0705147104
- Morales, J., Kadota, Y., Zipfel, C., Molina, A., and Torres, M.-A. (2016). The Arabidopsis NADPH oxidases *RbohD* and *RbohF* display differential expression patterns and contributions during plant immunity. *J. Exp. Bot.* 67, 1663–1676. doi: 10.1093/jxb/erv558
- Ngou, B. P. M., Heal, R., Wyler, M., Schmid, M. W., and Jones, J. D. G. (2022). Concerted expansion and contraction of immune receptor gene repertoires in plant genomes. *Nat. Plants* 8, 1146–1152. doi: 10.1038/s41477-022-01260-5
- Nitsch, J. P., and Nitsch, C. (1969). Haploid plants from pollen grains. Science 163, 85–87. doi: 10.1126/science.163.3862.85
- Pathak, V. M., Verma, V. K., Rawat, B. S., Kaur, B., Babu, N., Sharma, A., et al. (2022). Current status of pesticide effects on environment, human health and it's eco-friendly management as bioremediation: A comprehensive review. Front. Microbiol. 13, 962619. doi: 10.3389/fmicb.2022.962619
- Qiu, W., Feechan, A., and Dry, I. (2015). Current understanding of grapevine defense mechanisms against the biotrophic fungus (Erysiphe necator), the causal agent of powdery mildew disease. *Hortic. Res.* 2, 15020. doi: 10.1038/hortres.2015.20
- Rahman, M. U., Liu, X., Wang, X., and Fan, B. (2024). Grapevine gray mold disease: infection, defense and management. *Hortic. Res.* 11, uhae182. doi: 10.1093/hr/uhae182
- Roudaire, T., Marzari, T., Landry, D., Löffelhardt, B., Gust, A. A., Jermakow, A., et al. (2023). The grapevine LysM receptor-like kinase VvLYK5-1 recognizes chitin oligomers through its association with VvLYK1-1. *Front. Plant Sci.* 14, 1130782. doi: 10.3389/fpls.2023.1130782
- Ruijter, J. M., Ramakers, C., Hoogaars, W. M. H., Karlen, Y., Bakker, O., Van Den Hoff, M. J. B., et al. (2009). Amplification efficiency: linking baseline and bias in the analysis of quantitative PCR data. *Nucleic Acids Res.* 37, e45–e45. doi: 10.1093/nar/gkp045
- Shimada, T. L., Shimada, T., and Hara-Nishimura, I. (2010). A rapid and non-destructive screenable marker, FAST, for identifying transformed seeds of *Arabidopsis thaliana*. *Plant J.* 61, 519–528. doi: 10.1111/j.1365-313X.2009.04060.x
- Shimizu, T., Nakano, T., Takamizawa, D., Desaki, Y., Ishii-Minami, N., Nishizawa, Y., et al. (2010). Two LysM receptor molecules, CEBiP and OsCERK1, cooperatively

- regulate chitin elicitor signaling in rice: LysM receptors for rice chitin signaling. Plant J. 64, 204–214. doi: 10.1111/j.1365-313X.2010.04324.x
- Silva, C. J., Van Den Abeele, C., Ortega-Salazar, I., Papin, V., Adaskaveg, J. A., Wang, D., et al. (2021). Host susceptibility factors render ripe tomato fruit vulnerable to fungal disease despite active immune responses. *J. Exp. Bot.* 72, 2696–2709. doi: 10.1093/jxb/eraa601
- Spoel, S. H., Koornneef, A., Claessens, S. M. C., Korzelius, J. P., Van Pelt, J. A., Mueller, M. J., et al. (2003). NPR1 modulates cross-talk between Salicylate- and Jasmonate-Dependent defense pathways through a novel function in the cytosol. *Plant Cell* 15, 760–770. doi: 10.1105/tpc.009159
- Trdá, L., Fernandez, O., Boutrot, F., Héloir, M., Kelloniemi, J., Daire, X., et al. (2014). The grapevine flagellin receptor VvFLS2 differentially recognizes flagellin-derived epitopes from the endophytic growth-promoting bacterium *Burkholderia phytofirmans* and plant pathogenic bacteria. *New Phytol.* 201, 1371–1384. doi: 10.1111/nph.12592
- Vetter, M. M., Kronholm, I., He, F., Haweker, H., Reymond, M., Bergelson, J., et al. (2012). Flagellin perception varies quantitatively in *Arabidopsis thalia*na and its relatives. *Mol. Biol. Evol.* 29, 1655–1667. doi: 10.1093/molbev/mss011
- Wan, J., Tanaka, K., Zhang, X.-C., Son, G. H., Brechenmacher, L., Nguyen, T. H. N., et al. (2012). LYK4, a Lysin Motif Receptor-Like Kinase, is important for chitin signaling and plant innate immunity in Arabidopsis. *Plant Physiol.* 160, 396–406. doi: 10.1104/pp.112.201699
- Wang, T., Gasciolli, V., Gaston, M., Medioni, L., Cumener, M., Buendia, L., et al. (2023). LysM receptor-like kinases involved in immunity perceive lipochitooligosaccharides in mycotrophic plants. *Plant Physiol.* 192, 1435–1448. doi: 10.1093/plphys/kiad059
- Xiao, H., Liu, Z., Wang, N., Long, Q., Cao, S., Huang, G., et al. (2023). Adaptive and maladaptive introgression in grapevine domestication. *Proc. Natl. Acad. Sci. U.S.A.* 120, e2222041120. doi: 10.1073/pnas.2222041120
- Xu, L., Wang, J., Xiao, Y., Han, Z., and Chai, J. (2023). Structural insight into chitin perception by chitin elicitor receptor kinase 1 of *Oryza sativa*. *JIPB* 65, 235–248. doi: 10.1111/jipb.13279
- Xue, D.-X., Li, C.-L., Xie, Z.-P., and Staehelin, C. (2019). LYK4 is a component of a tripartite chitin receptor complex in *Arabidopsis thaliana*. *J. Exp. Bot.* 70, 5507–5516. doi: 10.1093/jxb/erz313
- Zaidi, S. S.-A., Mukhtar, M. S., and Mansoor, S. (2018). Genome editing: targeting susceptibility genes for plant disease resistance. *Trends Biotechnol.* 36, 898–906. doi: 10.1016/j.tibtech.2018.04.005
- Zhang, C., He, J., Dai, H., Wang, G., Zhang, X., Wang, C., et al. (2021). Discriminating symbiosis and immunity signals by receptor competition in rice. *Proc. Natl. Acad. Sci. U.S.A.* 118, e2023738118. doi: 10.1073/pnas.2023738118
- Zhou, J.-M., and Zhang, Y. (2020). Plant immunity: Danger perception and signaling. Cell 181, 978–989. doi: 10.1016/j.cell.2020.04.028
- Zimmerli, L., Métraux, J.-P., and Mauch-Mani, B. (2001). β -Aminobutyric acid-induced protection of Arabidopsis against the necrotrophic fungus *Botrytis cinerea*. *Plant Physiol.* 126, 517–523. doi: 10.1104/pp.126.2.517
- Zipfel, C. (2014). Plant pattern-recognition receptors. $Trends\ Immunol.\ 35, 345-351.$ doi: 10.1016/j.it.2014.05.004
- Zouine, M., Maza, E., Djari, A., Lauvernier, M., Frasse, P., Smouni, A., et al. (2017). TomExpress, a unified tomato RNA-Seq platform for visualization of expression data, clustering and correlation networks. *Plant J.* 92, 727–735. doi: 10.1111/tpj.13711